Weakly damped acoustic-like ion waves in plasmas with non-Maxwellian ion distributions

H. Gunell* and F. Skiff

Department of Physics and Astronomy, University of Iowa, Iowa City, Iowa 52242

Dispersion relations for ion-acoustic-like waves in plasmas with and without superthermal particles are calculated using a simple pole expansion of the distribution function for the ions. It is found that slow weakly damped modes exist in two-temperature plasmas, and the conditions when these modes appear are investigated. For plasmas with equal ion and electron temperatures weakly damped modes are found when there is a depletion of the high energy tails.

PACS numbers: 52.35.Fp

I. INTRODUCTION

Observations of non-Maxwellian ion velocity distributions in space have been reported by a number of authors, both in the earth's plasma sheet[1,2], in the solar wind[3], and elsewhere. The observed distribution functions contain a plentiful supply of superthermal particles, i.e., particles that are faster than the thermal speed. These are seen as high energy tails having a power-law dependence on velocity, and can often be modelled by kappa (or generalized Lorentzian) distributions. It is not unusual that a close fit to the observational data requires that the model consists of a sum of kappa distributions of equal or different temperatures centred at equal or different velocities.

Normal modes and instabilities for plasmas containing superthermal particles can be studied through the use of a plasma dispersion function for the kappa distribution[4,5]. Summers and Thorne[4] introduced a plasma dispersion function for the kappa distribution, valid for integer values of κ. This was generalized by Mace and Hellberg[5] to include any real value of κ. The Debye length for a kappa distribution has been calculated by Bryant[6]. Mace, Hellberg, and Treumann found that plasmas with superthermal particles have higher levels of electrostatic fluctuations and shorter Debye lengths than plasmas with Maxwellian velocity distributions[7]. The damping of the normal modes at high phase velocities is stronger for plasmas with superthermal particles than for Maxwellian plasmas[8]. It has been shown that the existence of ion acoustic instabilities is strongly influenced by the particle distribution functions[9].

Löfgren and Gunell developed a method for computation of dispersion relations for simple pole expansions of distribution functions[10]. The expansion is a rational function of the complex phase velocity v_{ph}, and the integration along the real axis is reduced to a sum of the residues at the poles of the expansion of the distribution function. Similar expansions were later used by Nakamura and Hoshino to study relativistic cyclotron resonances[11].

In this work a modified version of the scheme[10] is developed and used to find the normal modes for waves on the ion acoustic time scale. The derivation is based on the definition of the Debye length. The electrons can have any symmetric distribution function, and it is not necessary to assume a Maxwellian. In section II the method of calculating dispersion relations for ion waves for simple pole expansions of ion distribution functions is developed. In section III this method is applied to sound waves for one component distribution with and without superthermal tails. Dispersion relations for two-component distributions where the two components are centred at different velocities are studied in section IV. Distributions with two different temperatures are investigated in section V, and in section VI the results are summarized.

II. DISPERSION RELATIONS FOR ION ACOUSTIC WAVES

In this section an expression for the Debye length for the simple pole expansions is derived, and the expression obtained for the electron Debye length is used to express the dispersion relation for ion waves.

The dimensionless description introduced by Löfgren and Gunell[10] is

$$f(x) = M(x)T(x), \qquad x \equiv (v - v_d)/v_t$$

$$M(x) = \left[1 + \frac{x^2}{2} + \ldots + \frac{1}{m!}(\frac{x^2}{2})^m\right]^{-1} \tag{1}$$

$$T(x) = \left[1 + (\frac{x}{x_0})^{2n}\right]^{-1},$$

where M is 1 over a truncated Taylor expansion (about $x = 0$) of $e^{x^2/2}$ and T is a mask with critical velocity x_0, that can be used to introduce a cutoff in the high energy tails. The average drift speed is v_d and v_t is the standard deviation of the limiting Maxwellian. Note that this, v_t, is not the exact measure corresponding to the mean energy for distributions with truncated or thick tails. The distribution function given by Eq. (1) can be expressed as a sum of partial fractions $\sum_i a_i/(x - b_i)$, where a_i are the residues of the distribution function f at its poles b_i. For clarity and to be consistent with the previous paper[10] normalized variables with correct dimen-

sions will be used. The normalized distribution function is $\tilde{f} = \sum_i \tilde{a}_i/(v - \tilde{b}_i)$, where $\tilde{a}_i = a_i(2\pi i \sum_{b_i \in U} a_i)^{-1}$ and $\tilde{b}_i = b_i v_t + v_d$. U denotes the upper half plane. The Debye length can be defined[12] as $\lambda_D = \left(\sum_\alpha \lambda_{D\alpha}^{-2}\right)^{-1/2}$, where α denotes the different particle species and the Debye length for a single species is[12]

$$\lambda_{D\alpha} = \left(-\omega_{p\alpha}^2 \int dv \frac{1}{v}\frac{\partial}{\partial v} f_\alpha(v)\right)^{-1/2}. \qquad (2)$$

For a distribution function that is symmetric around $v = 0$ the following holds for the integrand of Eq. (2).

$$\frac{1}{v}\frac{\partial}{\partial v}f_\alpha(v) = \frac{1}{v}\frac{\partial}{\partial v}\left(\sum_{i=1}^{2m}\frac{\tilde{a}_{\alpha i}}{v - \tilde{b}_{\alpha i}}\right)$$

$$= -\frac{1}{v}\sum_{i=1}^{2m}\frac{\tilde{a}_{\alpha i}}{(v-\tilde{b}_{\alpha i})^2} = -\sum_{\tilde{b}_{\alpha i}\in U}\frac{4\tilde{a}_{\alpha i}\tilde{b}_{\alpha i}}{(v-\tilde{b}_{\alpha i})^2(v+\tilde{b}_{\alpha i})^2}, \qquad (3)$$

In the last step we have used the property of a distribution function that is symmetric around $v = 0$ that for every pole $\tilde{b}_{\alpha i} \in U$ with residue $\tilde{a}_{\alpha i}$ there is a pole $-\tilde{b}_{\alpha i}$ in the lower half plane with residue $-\tilde{a}_{\alpha i}$. The integration is performed using the residue theorem.

$$\frac{1}{\lambda_{D\alpha}^2} = -\omega_{p\alpha}^2\left(-2\pi i\sum_{\tilde{b}_{\alpha i}\in U}(-2)\frac{4\tilde{a}_{\alpha i}\tilde{b}_{\alpha i}}{(2\tilde{b}_{\alpha i})^3}\right)$$

$$= -\omega_{p\alpha}^2 2\pi i\sum_{\tilde{b}_{\alpha i}\in U}\frac{\tilde{a}_{\alpha i}}{\tilde{b}_{\alpha i}^2} \qquad (4)$$

When $\tilde{b}_{\alpha i}$ and $\tilde{a}_{\alpha i}$ are the poles and residues of an expansion of the Maxwellian the Debye length of Eq. (4) will approach the Debye length of the Maxwellian as m tends to infinity. A comparison between the Maxwellian Debye length and the Debye length for the expansion of Eq. (1) is shown in table I for various values of m and $n = 0$. Since $T = 1$ follows from $n = 0$ there is no high velocity cutoff in the tails. The moments $\langle v^q \rangle = \int_{-\infty}^{\infty} fv^q dv$ of the distribution function converge for $q < 2m + 2n - 1$, and by closing the contour of integration in the upper half plane U they have been found[10] to be $\langle v^q \rangle = \sum_{\tilde{b}_i \in U} \tilde{a}_i \tilde{b}_i^q$. In the calculation of λ_{Dm}/λ_D the thermal velocity for the unapproximated Maxwellian is chosen such that both distributions have the same second moment $\langle v^2 \rangle = \sum_{\tilde{b}_i \in U} \tilde{a}_i \tilde{b}_i^2$, that is

$$\tilde{f}_{Maxw}(v) = \frac{1}{\sqrt{\langle v^2 \rangle 2\pi}} \cdot e^{-\frac{v^2}{2\langle v^2 \rangle}}.$$

The thermal velocity v_t as it is defined here does not exactly represent the standard deviation of the distribution function $\tilde{f}$[10]. For small values of m, i.e., for distributions with an abundance of superthermal particles, the Debye length is significantly smaller than the Debye length of

TABLE I: Debye length λ_{Dm} according to Eq. (4) for expansions found in Eq. (1), for $m = 1, 2, \ldots 10$, $n = 0$, are compared with the Debye length λ_D for a Maxwellian that has the same second moment $\langle v^2 \rangle = \sum_{\tilde{b}_i \in U} \tilde{a}_i \tilde{b}_i^2$ as the expansion.

m	$\langle (v/v_t)^2 \rangle$	λ_{Dm}/λ_D
2	2.828	0.6436
3	1.376	0.8750
4	1.137	0.9469
5	1.059	0.9756
6	1.027	0.9884
7	1.013	0.9943
8	1.006	0.9972
9	1.003	0.9986
10	1.002	0.9993

the corresponding Maxwellian. Similar results have been obtained for a kappa-distribution with a small value of kappa[6,7].

In a multi-component plasma the dispersion relation is obtained by summarizing the contributions of the different components to Poisson's equation. In general the dispersion relation for a multi-component plasma is

$$1 = \int_{-\infty}^{\infty}\frac{\sum_\alpha \omega_{p\alpha}^2 \tilde{f}_\alpha}{(\omega - kv)^2}dv, \qquad (5)$$

where each component is normalized so that $\int_{-\infty}^{\infty}\tilde{f}_\alpha dv = 1$, and the total plasma frequency is obtained from the plasma frequency of the components by $\omega_p^2 = \sum_\alpha \omega_{p\alpha}^2$. For distribution functions expressed as simple pole expansions the dispersion relation is obtained by closing the contour of integration in the upper half plane[10]. For a plasma consisting of electrons and ions with distribution functions described by simple pole expansions Eq. (5) becomes

$$1 = \omega_{pi}^2 2\pi i\sum_{\tilde{b}_{ii}\in U}\frac{\tilde{a}_{ii}}{(\omega - k\tilde{b}_{ii})^2} + \omega_{pe}^2 2\pi i\sum_{\tilde{b}_{ei}\in U}\frac{\tilde{a}_{ei}}{(\omega - k\tilde{b}_{ei})^2}, \qquad (6)$$

where the first letter in the subscripts of $\tilde{a}$ and $\tilde{b}$ denotes particle species, i for ion and e for electron. The modulus of the poles $|\tilde{b}_{ei}|$ of the electron distribution function is on the order of the electron thermal speed. Thus for ion acoustic waves the modulus of the phase velocity $|\omega/k|$ is much less than the modulus of the poles $|\tilde{b}_{ei}|$. That this condition is met can be checked a posteriori. Hence the last term of Eq. (6) is approximately $-1/(k^2\lambda_{De}^2)$, and the dispersion relation becomes

$$1 = \omega_{pi}^2 2\pi i\frac{1}{1 + \frac{1}{k^2\lambda_{De}^2}}\sum_{\tilde{b}_i\in U}\frac{\tilde{a}_i}{(\omega - k\tilde{b}_i)^2}. \qquad (7)$$

In Eq. (7) the first index i has been omitted since all residues and poles now refer to the ion distribution function. If a Maxwellian velocity distribution is assumed for

the electrons the Debye length $\lambda_{De} = (\epsilon_0 k_\mathrm{B} T_\mathrm{e}/n_0 q^2)^{1/2}$ that is associated with the Maxwellian can be used. However, when the distribution function is non-Maxwellian but symmetric the Debye length given by Eq. (4) is more appropriate. The dispersion relation can be written as a polynomial in ω/k for a given $k \neq 0$.

$$\prod_i \left(\frac{\omega}{k} - \tilde{b}_i\right)^2 - \frac{\omega_{pi}^2}{k^2}\frac{1}{1 + \frac{1}{k^2\lambda_{De}^2}}2\pi i \sum_i \tilde{a}_i \prod_{j \neq i}\left(\frac{\omega}{k} - \tilde{b}_j\right)^2 = 0 \tag{8}$$

where the notation $\tilde{b}_i, \tilde{b}_j \in U$, i.e., restriction to the upper half plane, has been omitted in the summation and the products. The difference between Eq. (8) and Löfgren and Gunell's[10] Eq. (7)

$$\prod_i \left(\frac{\omega}{k} - \tilde{b}_i\right)^2 - \frac{\omega_p^2}{k^2}2\pi i \sum_i \tilde{a}_i \prod_{j \neq i}\left(\frac{\omega}{k} - \tilde{b}_j\right)^2 = 0$$

is the appearance of the new factor $1/(1 + 1/k^2\lambda_{De}^2)$ in the second term on the left hand side of Eq. (8) of the present paper. The dispersion relation can be found from Eq. (8) by polynomial root finders in standard numerical packages.

III. SOUND WAVES FOR NON-MAXWELLIAN ONE-COMPONENT DISTRIBUTIONS

In many plasmas the ion distribution is Maxwellian at low velocities, but deviate from the Maxwellian at higher velocities due to the velocity dependence of the collision frequency. The tail of the distribution function is important for the behaviour of ion acoustic waves, for which the phase velocity often is much higher than the thermal velocity.

An expansion according to Eq. (1) is a good approximation of the Maxwellian at low velocities, but shows increased tails at higher velocities, and can hence be a good approximation to plasmas containing superthermal particles. The normalized distribution function $\tilde{f}_0(v) = f_0(v)/n_0$ for $m = 2$ (dashed curves) and 5 (solid curves), $n = 0$, is shown in the upper panel of Fig. 1. $T = 1$ for $n = 0$ and there is no high velocity cutoff in the tails. Root paths in the complex phase-velocity space for these distribution functions, have been calculated using the method described in section II and are shown in the lower panel of Fig. 1. The long wavelength limits $(k \to 0)$ are marked with stars. As k is increased from zero the roots follow the paths shown and end at a pole of the distribution function as k tends to infinity. The poles are marked with circles. The weakly damped modes are found close to the real axis, and for these distribution functions they can be identified as the ion acoustic waves. For each of the distributions there is one ion acoustic mode propagating in the direction of positive v and one propagating in the direction of negative v. The dash-dotted lines starting at the origin show the border
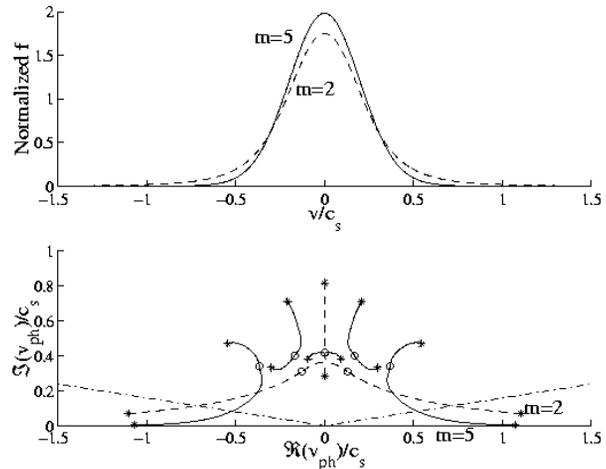

FIG. 1: Expansions of the normalized Maxwellian for $m = 2$ (dashed lines) and 5 (solid lines) are shown in the upper panel. The velocities are normalized to the sound speed $c_s = \sqrt{k_B T_e/m_i}$. The ion thermal speed is $v_{ti} = 0.2c_s$. The lower panel shows root paths in the complex phase velocity plane for these distribution functions. The poles of the distribution function are marked with circles and the limiting solutions $k \to 0$ are marked with stars. For high values of m the classic ion acoustic wave is obtained. For lower m-values the waves are more damped due to the presence of particles in the tails close to the phase velocity of the wave. Wave modes below the dash-dotted lines in the lower panels fulfill the condition $\Im(\omega)/|\Re(\omega)| < 1/(2\pi)$ and are considered to be weakly damped.

between the weakly and heavily damped regions, with the weakly damped region being below the lines. The criterion used for a wave mode being weakly damped is that the imaginary part of ω shall be less than the real part divided by 2π, i. e., $\Im(\omega)/|\Re(\omega)| < 1/(2\pi)$. In Fig. 2 the real (upper panel) and imaginary (lower panel) parts of ω are shown as a function of k for the ion acoustic mode travelling in the direction of positive v. The dispersion relations are shown for distributions with $m = 1, 2, 3, 4$, and 5. Only for the Lorentzian $(m = 1)$ is there any significant deviation of the real part of ω from what a true Maxwellian would yield. In the lower panel, however it is seen that superthermal particles contribute significantly to the imaginary part of ω making the wave more damped for small values of m.

The increased damping for non-Maxwellian distributions can be understood as a contribution by the larger number of particles in the tails close to the phase velocity of the wave, where there are very few particles in a Maxwellian plasma. Landau damping is proportional to the slope of the distribution function in the neighbourhood of the phase velocity of the wave. Because of this the increased damping also is due to the derivative $|\partial f_0/\partial v|$ that is exceptionally small for a Maxwellian. For a Maxwellian the $\partial f_0/\partial v$ is proportional
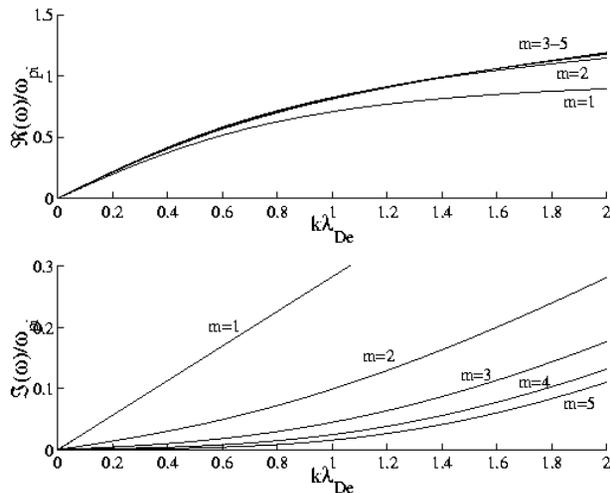
FIG. 2: Dispersion relation for the ion acoustic wave travelling in the positive v direction. The real part of ω is shown in the upper panel as a function of k. The lower panel show the imaginary part of ω as a function of k. The dispersion relations are shown for distribution functions with $n = 0$ and $m = 1, 2, 3, 4$, and 5.
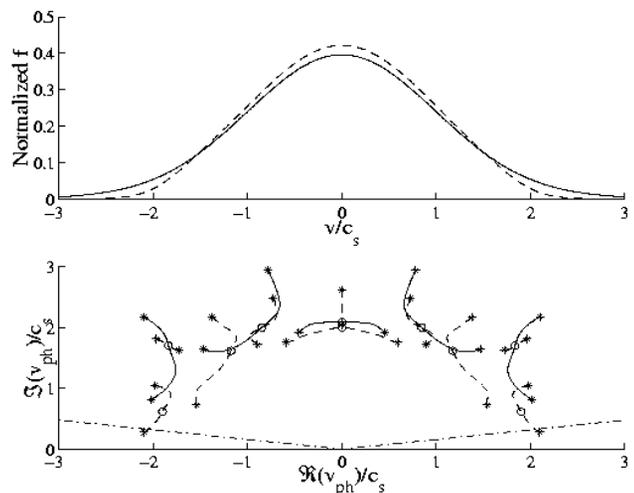

FIG. 3: Upper panel: $m = 5$ expansion of a Maxwellian with $T_i = T_e$ (solid line) and the same function with a gentle cutoff introduced at $v = 2c_s$. Lower panel: Root paths in the complex phase velocity space for these distributions. The poles of the distribution functions are marked with circles and the limiting solutions $k \to 0$ are marked with stars. Wave modes below the dash-dotted lines in the lower panels fulfill the condition $\Im(\omega)/|\Re(\omega)| < 1/(2\pi)$ and are considered to be weakly damped.

to $-v \cdot \exp(-v^2/2v_t^2)$ for large $|v|$, whereas $\partial f_0/\partial v$ for the expansions used here is proportional to $-|v|^{-(2m+1)}$ for large $|v|$.

A cutoff in the tail of the distribution can be introduced by setting $n \neq 0$ in Eq. (1). This is equivalent to a multiplication of the expansion with the transfer function of a low-pass Butterworth filter. In Fig. 3 an example of the introduction of a gentle cutoff is shown. In the upper panel the solid line shows an $m = 5$, $n = 0$ expansion of a Maxwellian distribution function with $T_i = T_e$. The dashed line shows an $m = 5$, $n = 5$ expansion, i.e., the same distribution multiplied by $T(v) = (1 + (v/v_c)^{10})^{-1}$, which is the square of the modulus of the transfer function for a fifth order Butterworth low-pass filter. Here v_c is the cutoff velocity which in the example shown in Fig. 3 is $2c_s$. This distribution has less ions in the high energy tails. Such a distribution function could be produced in the presence of neutral gas, since the collision frequency for charge-exchange collisions increases with energy. Root paths in the complex phase velocity space for these two distribution functions are shown in the lower panel of Fig. 3. As expected the Maxwellian plasma with $T_i = T_e$ (solid lines) has only heavily damped modes. For the distribution with the cutoff tails (dashed lines) there is a weakly damped mode with a phase velocity close to $2.1c_s$, which is slightly faster than the cutoff velocity $v_c = 2c_s$. This mode is an acoustic mode since, as can be seen in Fig. 3, it has an approximately constant phase speed in the $k \to 0$ limit, which is marked with a star, and hence ω is proportional to k in that limit. It is not, however, a traditional ion acoustic wave as its phase speed is twice the ion sound speed. The introduction of a cutoff acts to decrease the damping at velocities above the cut-

off since both the slope of the distribution function and the number of particles in that velocity range decreases when the cutoff is introduced, and Landau damping is proportional to the slope of the distribution function in the neighbourhood of the phase velocity. In this way the presence of charge exchange collisions could decrease the damping rate. The criterion used to determine whether a wave mode is weakly or heavily damped is that a weakly damped mode shall have $\Im(\omega)/|\Re(\omega)| < 1/(2\pi)$. The weakly damped modes are in the region below the dash-dotted lines in Fig. 3.

IV. TWO-COMPONENT DISTRIBUTIONS WITH BEAM-LIKE TAILS

Many ion distribution functions in naturally occurring plasmas can be modeled by a sum of expansions with different temperature centred at different velocities. Here a beam-like distribution function is studied, i.e., a distribution in which most of the ions belong to a population centred at zero velocity and a fraction of the ions belong to an enhanced tail that can be modeled by an expansion centred at non-zero velocity. Such ion distribution functions have been observed in laboratory plasmas and have been found to carry both classic ion acoustic waves and slow kinetic wave modes[13].

In the upper panel of Fig. 4 three beam-like distributions can be seen. The relative density η of the beam (or enhanced tail) is equal to the ratio of the square of
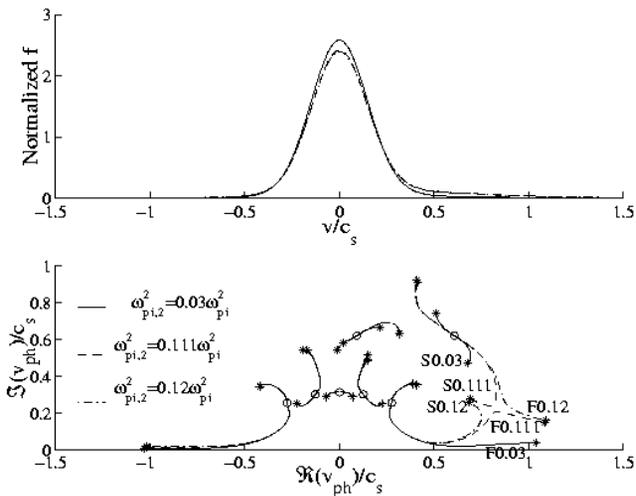
FIG. 4: Distribution functions (upper panel) and root paths (lower panel) for three beam-like distributions. The poles of the distribution function are marked with circles and the limiting solutions $k \to 0$ are marked with stars. The solid lines show the case where the relative beam (or enhanced tail) density $\eta = \omega_{pi,2}^2/\omega_{pi}^2 = 0.03$. For the dashed lines $\eta = 0.111$ and for the dash-dotted lines $\eta = 0.12$. The labels on some of the root paths also appear in Fig. 5 at the corresponding dispersion relations. In the labels S means slow, F means fast and the numbers refer to the relative tail density η. The parameters are found in table II.

TABLE II: Parameters of the distribution functions shown in Fig. 4 The total ion plasma frequency ω_{pi} and the sound speed c_s are used as scaling parameters. The background plasma has index 1 and the tail 2.

line	$\omega_{pi,1}^2$	$v_{ti,1}$	$v_{d,1}$	m_1	$\omega_{pi,2}^2$	$v_{ti,2}$	$v_{d,2}$	m_2
—	$0.97\omega_{pi}^2$	$0.15c_s$	0	5	$0.03\omega_{pi}^2$	$0.4c_s$	$0.35c_s$	2
- -	$0.889\omega_{pi}^2$	$0.15c_s$	0	5	$0.111\omega_{pi}^2$	$0.4c_s$	$0.35c_s$	2
-.-	$0.88\omega_{pi}^2$	$0.15c_s$	0	5	$0.12\omega_{pi}^2$	$0.4c_s$	$0.35c_s$	2

the beam plasma frequency to the square of the total ion plasma frequency. In Fig. 4 $\eta = \omega_{pi,2}^2/\omega_{pi}^2 = 0.03$ for the solid curve, $\eta = 0.111$ for the dashed curve, and $\eta = 0.12$ for the dash-dotted curve. The tail distribution is centred about $v_0 = 0.35c_s$. The parameters of the distribution functions are shown in table II. In the lower panel of Fig. 4 root paths for the three distributions are shown. The poles of the distribution functions are shown as circles. The two uppermost poles (at $\Im(v_{ph})/c_s \approx 0.6$) belong to the tail distribution and the lower five poles that are centred around $\Re(v_{ph}) = 0$ belong to the bulk plasma distribution. When the relative tail density η is varied the residues change but the poles remain the same. The root paths start at the stars that mark the long wavelength limit ($k \to 0$) and for increasing values of k the roots move along the shown curves and end at one of the poles in the short wave length limit ($k \to \infty$). The root paths discussed below have been labeled S0.03, S0.111, S0.12,
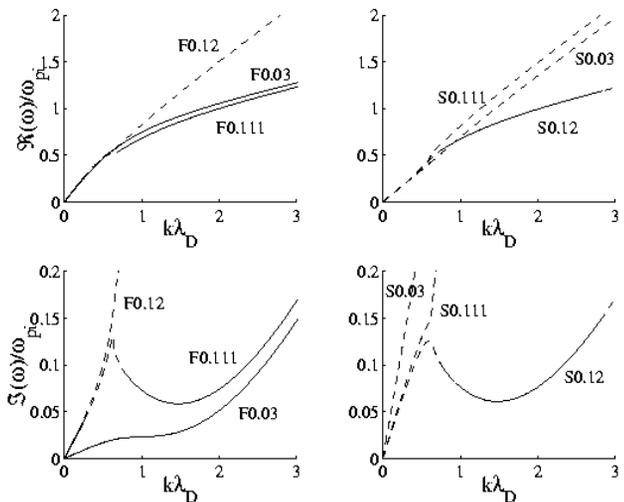
FIG. 5: Dispersion relations for the distribution functions of Fig. 4. The upper panels show $\Re(\omega)$ and the lower panels $\Im(\omega)$, both as a function of k. The faster wave modes are shown in the left panels and the slow modes are shown in the right panels. The lines are solid where the damping is weak ($\Im(\omega)/|\Re(\omega)| < 1/(2\pi)$) and dashed where the damping is strong. The labels are the same as on the corresponding root paths in Fig. 4.

F0.03, F0.111, and F0.12 respectively, where S means slow, F means fast, and the numbers refer to the relative tail density η. The two distributions with higher tail density are nearly identical, and hence these curves, in the upper panel of Fig. 4, are almost on top of each other. Although the distribution functions are almost equal the root paths for $\eta = 0.11$ and $\eta = 0.12$ are distinctly different, as the lower panel of Fig. 4 shows. As the relative tail density increases from 0.111 to 0.12 a topological shift occurs, and the ion acoustic mode (F0.111) that for low tail density is connected to a pole of the bulk plasma distribution in stead becomes F0.12, that is connected to one of the poles of the tail. Dispersion relations for these modes are shown in Fig. 5. The upper panels show $\Re(\omega)$ and the lower panels $\Im(\omega)$. The left panels show the wave modes that are faster in the $k \to 0$ limit, and the right panels show wave modes that are slower in that limit. The parts of the wave modes that are weakly damped ($\Im(\omega)/\Re(\omega) < 1/(2\pi)$) are shown as solid lines and the strongly damped ($\Im(\omega)/\Re(\omega) > 1/(2\pi)$) parts are shown as dashed lines. The curves have labels as their corresponding curves in Fig. 4.

All modes shown in Fig. 5 have a constant phase velocity for small k and are hence acoustic-like in their behaviour. The mode labeled F0.03 in the left hand panels is the traditional ion acoustic mode, and it is the only weakly damped mode in the case with the lowest tail density. As the tail density is increased this mode will become mode F0.111 that is weakly damped at small k, strongly damped at intermediate values of k, and have another weakly damped region for larger k. This is the

continuous transition from the F0.03 curve to the F0.111 curve in the left panels of Fig. 5. It can also be seen in the lower panel of Fig. 4, where when the η increases from 0.03 to 0.111 the solid curve (F0.03) goes through a continuous transition to the dashed curve (F0.111) which has a bump in the intermediate k region where the damping is strong.

When the tail density is 11.1% the only weakly damped mode in the positive v direction is the mode labeled F0.111. This mode is weakly damped for small and large k, and strongly damped for intermediate k. When the relative tail density is increased to 12% there are still weakly damped modes for these values of k, namely F0.12 is weakly damped for small k and S0.12 is weakly damped for larger k. The weakly damped regions, that are shown as solid curves in Fig. 5, change very little as the tail density increases from 11.1% to 12%. The topological shift that is seen in Fig. 4 occurs in a region of the complex phase velocity space (Fig. 4) where the damping is strong and that corresponds to an interval of k-values (Fig. 5) where the modes involved are strongly damped. The larger change that occurs in the strongly damped region will be more difficult to observe due to the strong damping. Topological shifts in strongly damped regions are not likely to be important experimentally, but the study of these can increase our understanding of the wave phenomena involved.

Linear kinetic wave modes differing from the traditional ion acoustic waves have been observed in laboratory experiments[13]. Although the distribution functions treated here are examples rather than close fits to a measured distribution the distribution functions in these experiments are similar in that they can be modeled by a two-component distribution with a non-Maxwellian beam-like tail centred at approximately $v_0 = 0.35c_s$.

V. TWO TEMPERATURE DISTRIBUTIONS

In a plasma where there are two ion populations with different temperature weakly damped modes similar to those reported in section IV exist under some conditions. To find what these conditions are an ion velocity distribution consisting of one hot and one cold component is studied here. The existence of weakly damped modes has been determined for various values of the thermal velocity of the cold component v_{tc}, the thermal velocity of the hot component v_{th}, the relative density of the hot ions $f = n_h/n_i$, and the number of poles m_c and m_h in the expansions of the cold and hot ion populations respectively. Both the ion species have the same mass. The notation m_c and m_h only refers only to the orders at which the distributions are truncated, m_c and m_h are not the ion masses.

The different kinds of wave modes that can exist are shown in Fig. 6. The upper panels show the distribution functions and the lower panels the root paths in the complex phase velocity space. In the example shown $m_c = 5$,
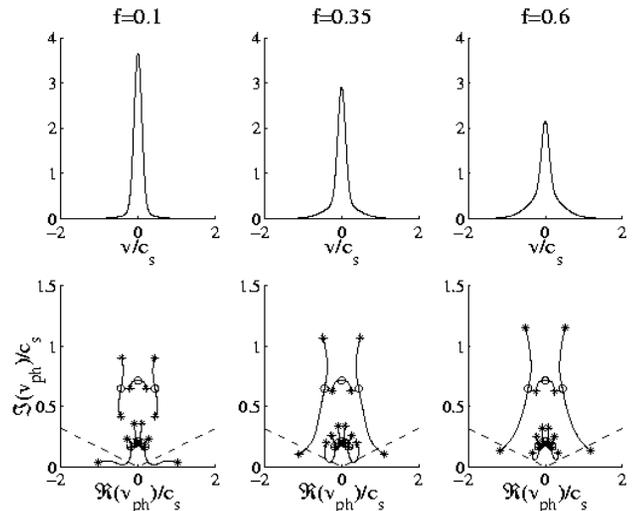

FIG. 6: The upper panels show the normalized distribution functions and the lower panels the root paths in the complex phase velocity space. The poles of the distribution function are marked with circles and the limiting solutions $k \to 0$ are marked with stars. Wave modes below the dashed lines in the lower panels fulfill the condition $\Im(\omega)/|\Re(\omega)| < 1/(2\pi)$ and are hence weakly damped. When $f = n_h/n_i = 0.1$ (left panels) the only weakly damped mode is the cold acoustic wave. For $f = n_h/n_i = 0.35$ (middle panels) the hot acoustic wave is weakly damped, and so is the slow (cold) wave for high values of k. At $f = n_h/n_i = 0.6$ the slow wave is heavily damped for all k and the hot acoustic wave is weakly damped. In all three cases $m_c = 5$, $v_{tc} = 0.1c_s$, $m_h = 3$, and $v_{th} = 0.4c_s$.

$v_{tc} = 0.1c_s$, $m_h = 3$, and $v_{th} = 0.4c_s$. For all distributions in this section $n = 0$, which means there is no high velocity cutoff in the tails of the distribution functions. The poles are shown as circles in the lower panels, and the three uppermost poles are the poles of the hot distribution. The group of five poles closer to the origin are the poles of the cold distribution. The dashed lines in the lower panels are the $\Im(\omega)/|\Re(\omega)| = 1/(2\pi)$ lines, that form the border between the weakly and strongly damped regions. Wave modes below the dashed lines are weakly damped and wave modes above the dashed lines are strongly damped. For low f the plasma ions are mostly cold and the cold ion acoustic wave is the only weakly damped wave mode. As is seen from the lower left panel of Fig. 6 the modes associated with the hot ion component are all in a very strongly damped region. In the long wavelength ($k \to 0$) limit, which is marked with a star, the root path of the cold ion acoustic wave starts near $v_{ph} = c_s$. For increasing k-values the root path follows the real axis in the weakly damped region and approaches a pole of the cold component distribution function in the short wavelength ($k \to \infty$) limit. The root paths of the cold ion acoustic wave are very similar to the root paths of the traditional ion acoustic wave that are shown in Fig. 1.

For high f values the dominant wave mode is the ion acoustic wave associated with the hot ion component. This is shown in the lower right panel of Fig. 6 for $f = 0.6$. The $k \to 0$ limit is in the weakly damped region of the complex phase velocity and the real part of the phase velocity is close to the ion acoustic velocity. This means that ω is proportional to k for small k and therefore the wave is acoustic, and since its velocity is close to the ion acoustic velocity it is identified as the ion acoustic wave. In the short wavelength limit the root path connects with a pole of the hot component distribution function. In this parameter regime all waves associated with the cold distribution are strongly damped. By comparing the left and the right of the lower panels it is seen that the damping is stronger in the $f = 0.6$ case than in the $f = 0.1$ case. This is to be expected because in the case with higher f there are more particles in the hot distribution and thus more particles in the neighbourhood of the phase velocity, as is seen in the upper panels of Fig. 6.

For intermediate values of f both the hot and cold waves can be weakly damped as the lower middle panel of Fig. 6, where $f = 0.35$, shows. The cold wave is strongly damped for small and very large k. Having a finite phase velocity in the long wavelength limit, but being in a strongly damped region of the complex phase velocity space in that limit, and only entering the weakly damped region for an interval of moderately large k, the wave associated with the cold plasma component is acoustic-like and very similar to the S0.12 mode shown in Fig. 4 and Fig. 5 for a distribution with beam-like tails. The hot plasma wave is weakly damped in the long wavelength limit and there has a phase velocity that is close to the ion sound speed, and thus it is an ion acoustic wave. It is in the weakly damped regime ($\Im(\omega) < \Re(\omega)/(2\pi)$) for $k\lambda_{De} \lesssim 0.6$.

If the hot ion component is so hot that $T_e = T_i$ there can still be weakly damped modes if a cold ion component is present, and even if that component constitutes only a small fraction of the total ion density. Fig. 7 shows two examples of this. The upper panels show the distribution functions and the lower panels show the root paths in the complex phase velocity space for plasmas with these ion distribution functions. In the left panels $f = 0.9$, $v_{tc} = 0.1c_s$ and $v_{th} = c_s$. The parameters of the distribution function shown in the upper right panel are $f = 0.6$, $v_{tc} = 0.2c_s$ and $v_{th} = c_s$. The three upper most poles shown in the lower panels are the poles of the hot component of the distribution, for which $v_{th} = c_s$, and hence $T_e = T_i$. The wave modes whose root paths connect to the poles of the hot distribution in the $k \to \infty$ limit are all heavily damped, as would be expected for waves in a plasma with equal electron and ion temperatures. In the presence of a cold plasma component there is a slow weakly damped acoustic wave mode. Its phase speed is lower than the ion sound speed. The slow wave is weakly damped even when the cold ion component only contributes to 10% of the total ion density, as is shown in
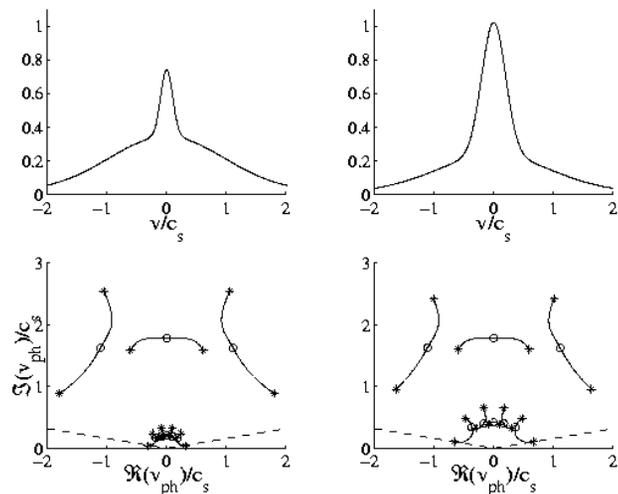

FIG. 7: Same as Fig. 6 except that the parameters are $f = 0.9$, $v_{tc} = 0.1c_s$, $v_{th} = c_s$ for the left panels and $f = 0.6$, $v_{tc} = 0.2c_s$, $v_{th} = c_s$ for the right panels.

the left panels of Fig. 7, where the thermal speed of the cold component is $v_{tc} = 0.1c_s$. The upper right panel of Fig. 7 shows a distribution function with a warmer cold component ($v_{tc} = 0.2c_s$). Here the cold component contributes to 40% of the total ion density. Also here a slow weakly damped mode is seen, but as the cold component is warmer a higher cold density, i. e., lower f, is required for the mode to be weakly damped.

Various parameters of two-temperature plasmas have been investigated to find parameter regimes where weakly damped modes can exist. Fig. 8 shows where weakly damped mode exist for a plasma with a cold ion component ($v_{tc} = 0.1c_s$) and a hot component with thermal speeds $v_{th}/c_s = 0.2$, 0.4, 0.6, 0.8, and 1.0 respectively. This figure and Fig. 9 have been obtained by numerically solving Eq. (8) and applying the weak damping condition $\Im(\omega) < \Re(\omega)/(2\pi)$. In the shadowed regions at least one mode is weakly damped. The shadowed region withdraws from the lower right quadrant of the diagrams as we go from the leftmost panel to the middle panel. This means that as the hot temperature increases the ion acoustic wave associated with the hot ion component gets more damped. Instead a shadow emerges from the upper left corner. This is the slow wave associated with the cold ions, which is weakly damped when v_{th} approaches c_s. The influence of superthermal particles is shown in Fig. 9. The cold ions follow a $v_{tc} = 0.03c_s$, $m_c = 5$ expansion, and the hot ions have $v_{th} = 0.3c_s$. The for panels correspond to $m_h = 1, 2, 3,$ and 4 from left to right. When m_h is increased from 1 to 4 the number of superthermal particles decreases and the damping of the ion acoustic mode decreases. This is seen in the diagrams in Fig. 9 where the shadowed region fills more and more of the lower half of this diagrams as we go from left to right, i. e, towards a lower number of superthermal
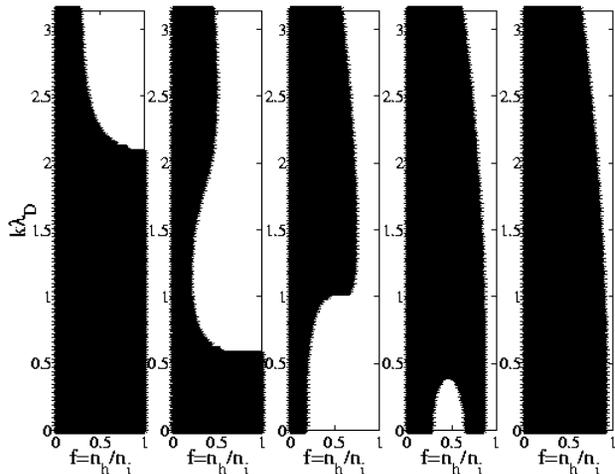
FIG. 8: The existence of weakly damped modes for different hot ion temperatures. In the shadowed regions weakly damped $(\Im(\omega)/\Re(\omega) < 1/(2\pi))$ modes exist. The cold ions follow a $v_{tc} = 0.1c_s$, $m_c = 5$ expansion, and the hot ions have $m_h = 3$, i.e., a distribution with some superthermal particles. The hot ion thermal speed $v_{th}/c_s = 0.2$, 0.4, 0.6, 0.8, and 1.0 respectively.
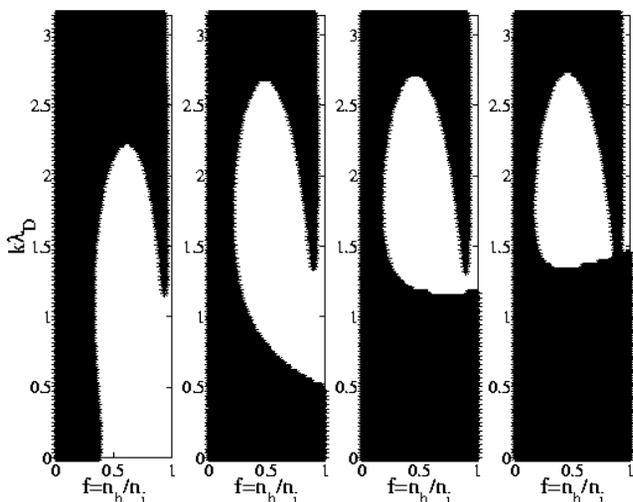

FIG. 9: The existence of weakly damped modes for different hot ion temperatures. In the shadowed regions weakly damped $(\Im(\omega)/\Re(\omega) < 1/(2\pi))$ modes exist. The cold ions follow a $v_{tc} = 0.03c_s$, $m_c = 5$ expansion, and the hot ions have $v_{th} = 0.3$. The number of superthermal particles decreases as m_h increases. In the four panels $m_h = 1, 2, 3$, and 4 from left to right.

particles. The existence of a slow mode associated with the cold component is not affected to any great extent of the presence of superthermal particles in the hot ion component.

VI. SUMMARY AND CONCLUSIONS

The existence of weakly damped modes in one and two ion component plasmas has been investigated in this pa-

per using a modified version of a previously published method for calculation of dispersion relations for plasmas where the particle velocity distribution functions can be written as simple pole expansions[10]. It is found that weakly damped modes with phase velocities lower than the ion acoustic velocity $\sqrt{k_B T_e/m_i}$ exist for a variety of two component distribution functions. Ion velocity distribution consisting of two components with different temperatures can support weakly damped modes even when the temperature of the hot component is equal to the electron temperature, and the hot ions constitute 90% of the total ion density. These modes are analogous to the higher-order modes found in plasmas with two ion species[14]. The reason for this similarity is that the quantity that is important for the dispersion relations is the thermal speed and hence the cold component in a two temperature plasma corresponds to the heavy component in a two ion species plasma. Similar waves appear on an electron time scale in plasmas with two electron temperatures where the weakly damped wave modes are the Langmuir and the electron acoustic waves[15–17].

A system with a stationary ion distribution and a low density tail centred at a velocity approximately equal to the thermal velocity show both the classical ion acoustic wave mode and slower acoustic-like modes that are strongly damped for low k-values and weakly damped in an interval of larger k. An example was given of how the dispersion relation changes as the relative density of the tail component changes. The observed slow mode is of the same kind as those that appear in two temperature plasmas with both distributions centred at the same velocity. The non-zero mean velocity of the tail decreases the damping of these modes.

In a plasma with a one-component ion distribution with $T_e = T_i$ weakly damped acoustic-like modes can exist at higher velocities if tail of the distribution is depleted, as it in some cases can be due to atomic processes.

The general question that yet remains unanswered is what characterizes a class of distribution functions that can support weakly damped wave modes. The approach taken here has been to study simple examples of distribution functions, and to vary the parameters to find when weakly damped modes occur. It is likely that most measured distribution functions can be reasonably well approximated by an expansion of the kind used in this paper. Dispersion relations can then easily be calculated and parameters varied also for more complicated functions.

* Electronic address: `herbert.gunell@physics.org`

[1] E. T. Sarris, S. M. Krimigis, A. T. Y. Lui, K. L. Ackerson, L. A. Frank, and D. J. Williams, Geophysical Research Letters **8**, 349 (1981).

[2] D. J. Williams, D. G. Mitchell, and S. P. Christon, Geophysical Research Letters **15**, 303 (1988).

[3] J. T. Gosling, J. R. Asbridge, S. J. Bame, W. C. Feldman, R. D. Zwickl, G. Paschmann, N. Sckopke, and R. J. Hynds, Journal of Geophysical Research **86**, 547 (1981).

[4] D. Summers and R. M. Thorne, Physics of Fluids B **3**, 1835 (1991).

[5] R. L. Mace and M. A. Hellberg, Physics of Plasmas **2**, 2098 (1995).

[6] D. A. Bryant, Journal of Plasma Physics **56**, 87 (1996).

[7] R. L. Mace, M. A. Hellberg, and R. A. Treumann, Journal of Plasma Physics **59**, 393 (1998).

[8] R. M. Thorne and D. Summers, Physics of Fluids B **3**, 2117 (1991).

[9] Z. Meng, R. M. Thorne, and D. Summers, Journal of Plasma Physics **47**, 445 (1992).

[10] T. Löfgren and H. Gunell, Physics of Plasmas **4**, 3469 (1997).

[11] T. K. Nakamura and M. Hoshino, Physics of Plasmas **5**, 3547 (1998).

[12] N. A. Krall and A. W. Trivelpiece, *Principles of Plasma Physics* (McGraw-Hill, New York, 1973).

[13] F. Skiff, S. De Souza-Machado, W. A. Noonan, A. Case, and T. N. Good, Physical Review Letters **81**, 5820 (1998).

[14] I. M. A. Gledhill and M. A. Hellberg, Journal of Plasma Physics **36**, 75 (1986).

[15] S. P. Gary and R. L. Tokar, Physics of Fluids **28**, 2439 (1985).

[16] R. L. Mace and M. A. Hellberg, Journal of Plasma Physics **43**, 239 (1990).

[17] R. L. Mace, G. Amery, and M. A. Hellberg, Physics of Plasmas **6**, 44 (1999).